INTERNATIONAL ATOMIC ENERGY AGENCY
UNITED NATIONS EDUCATIONAL, SCIENTIFIC AND CULTURAL ORGANIZATION
INTERNATIONAL CENTRE FOR THEORETICAL PHYSICS
I.C.T.P., P.O. BOX 586, 34100 TRIESTE, ITALY, CABLE: CENTRATOM TRIESTE

UNITED NATIONS INDUSTRIAL DEVELOPMENT ORGANIZATION

INTERNATIONAL CENTRE FOR SCIENCE AND HIGH TECHNOLOGY
c/o INTERNATIONAL CENTRE FOR THEORETICAL PHYSICS 34100 TRIESTE (ITALY) VIA GRIGNANO, 9 (ADRIATICO PALACE) P.O. BOX 586 TELEPHONE 040-224572 TELEFAX 040-224575 TELEX 460449 APH I

SMR/760-4

"College on Atmospheric Boundary Layer and Air Pollution Modelling"
16 May - 3 June 1994

"Hybrid Plume Dispersion Model (HPDM) Improvements and Testing at Three Field Sites"

S. HANNA
Environmental Research and Technology, Inc.
Concord, Massachusetts
USA

Please note: These notes are intended for internal distribution only.

Atmospheric Environment Vol. 27A, No. 9, pp. 1491–1508, 1993.
Printed in Great Britain.

0004-6891/93 $6.00 + 0.00

HYBRID PLUME DISPERSION MODEL (HPDM) IMPROVEMENTS AND TESTING AT THREE FIELD SITES

STEVEN R. HANNA and JOSEPH C. CHANG
Sigma Research Corporation, 196 Baker Avenue, Concord, MA 01742, U.S.A.

(*First received* 13 *May* 1992 *and in final form* 28 *October* 1992)

Abstract—Descriptions of several technical improvements to the Hybrid Plume Disperion Model (HPDM) are given. The boundary-layer meteorological preprocessor now makes use of a surface moisture availability parameter and now accounts for mechanical mixing due to buildings in urban areas. A new dispersion algorithm has been added in order to simulate conditions better when a buoyant plume "lofts" against the capping inversion and spreads laterally before dispersing down to the ground.

The modified model has been evaluated using 89 h of SF_6 tracer data at an urban power plant in Indianapolis, IN, and using a full year (8760 h) of SO_2 data at the Baldwin, IL, power plant and the Summit County, OH, industrial complex. The EPA's RAM and ISC models are also included in the evaluation exercises. Emphasis is on the second-highest concentrations, the correlation, the fractional mean bias and the fraction of predictions within a factor of two of observations for 1-, 3- and 24-h averaging times. The HPDM model exhibits significantly better performance (at the 95% confidence level) than the RAM or ISC model for most sites and performance measures. In most cases, the HPDM "second-highest" predictions are within 10–20% of the observations and the fractional mean bias values are less than 10%. Furthermore, the relative error of HPDM shows little trend with input variables such as wind speed and mixing depth.

Key words index: Dispersion modeling, boundary-layer, model evaluation, stack plume model.

1. INTRODUCTION

The Hybrid Plume Dispersion Model (HPDM) is intended for use in calculating hourly averaged ground-level concentrations of non-reacting gases released from industrial stacks. It incorporates state-of-the-art scientific features yet is sufficiently efficient and robust that it can be easily and confidently applied to thousands of hours of input data, dozens of sources and thousands of receptor locations. This paper describes the scientific components of the model and presents the results of its evaluation at three field sites.

Several modeling groups are developing new operational dispersion models similar to HPDM (e.g. the OML model described by Olesen, 1988; the AERMIC model described by Weil, 1992; and the ADMS model described by Carruthers *et al.*, 1992). These models will include improved surface heat and momentum flux parameterizations and employ principles of convective scaling and bimodal vertical velocity probability density functions during unstable conditions (e.g. Weil, 1988) and improved formulae for vertical profiles of winds, temperature and turbulence during stable conditions (e.g. Venkatram, 1988). However, the new models have received only limited testing with field data.

HPDM has a 10-year history. Hanna and Paine (1987, 1989) discuss an early version of the model, which was developed and evaluated using a few hundred hours of tracer data from two tall-stack sources in rural areas (the Kincaid, IL, and Bull Run, TN, power plants). Maximum ground-level concentrations at those sites were observed during light-wind convective conditions, when strong vertical convection rapidly mixed the elevated stack plume down to the ground. Because the stacks were so tall (about 180–200 m), the plumes seldom diffused to the ground with high concentrations during stable conditions. As a result, the model development efforts emphasized convective conditions.

Operational testing of the earlier version of HPDM at other sites and by many scientists and engineers in government agencies and in industrial plants for a variety of source scenarios revealed inadequacies during certain combinations of conditions. For example, at sites where stack heights were less than 100 m, high ground-level concentrations were as likely to be observed during stable or neutral conditions as during convective conditions. Dispersion under stable or neutral conditions was found to be not adequately simulated by HPDM. In addition, because the earlier version of HPDM did not account for changes in terrain height or for building obstacles, it was inapplicable to many sites. Furthermore, the question remained whether HPDM was valid in urban areas or other regions with large roughness elements and inhomogeneous surfaces.

Consequently, a three-pronged effort was begun in order to improve HPDM. First, a field program took place around an urban power-plant stack in Indianapolis, IN (TRC, 1986). Second, the scientific modules in HPDM were modified based on the results of the field program and based on recent theoretical developments. Third, the modified HPDM was evaluated with 1 year's worth of hourly operational data

from the Baldwin, IL, power-plant and from the Summit County, OH, industrial region. The results of the first two efforts are described in great detail in the three-volume project report by Hanna and Chang (1991). One section of the report, covering the revised boundary-layer parameterization schemes, is discussed in the article by Hanna and Chang (1992). The current paper emphasizes the dispersion algorithms in HPDM and presents the results of the evaluation of the model with the Indianapolis, Baldwin and Summit County field data. The various field data sets have been compiled into databases that are available on floppy disk from the Electric Power Research Institute's Atmospheric Sciences Data Center (EPRI-ASDC).*

2. OVERVIEW OF HPDM

Before describing the details of the technical algorithms (see Sections 3 and 4), it is useful to present an overview of the basic characteristics of HPDM. The latest version of the model is denoted HPDM 4.2.

Computer requirements: HPDM is available on a floppy disk and runs on a PC.

Input data: Hourly information for 1–50 stack sources can be input. Several types of hourly meteorological data can be input, ranging from routine National Weather Service (NWS) weather observations to detailed on-site observations of wind, temperature and turbulence profiles. Locations of up to 5000 receptors can be specified.

Output data: Complete binary hourly concentration files are available for all receptors and times, as well as data summaries similar to those produced by U.S. EPA models.

Meteorological preprocessor: The role of the meteorological preprocessor is to produce a file of hourly averaged surface heat fluxes and momentum fluxes (i.e. friction velocities), based on, for example, observations of wind speed and cloudiness and specification of surface roughness length, surface moisture availability and albedo. These surface fluxes, along with the mixing depth, then completely determine the vertical profiles of wind and turbulence.

HPDM dispersion algorithm: Given the surface fluxes and the stack conditions, the HPDM dispersion algorithm calculates hourly averaged ground-level concentrations, using the straight-line Gaussian plume model during stable and most neutral conditions, using the PDF model during unstable conditions when the plume does not rise to the mixing lid, using the "low-wind" model during unstable conditions when the plume impacts the mixing lid, and using the "lofting" model during neutral conditions when the plume impacts the mixing lid.

Building downwash: The dispersion coefficients are corrected for the effects of building downwash using methods consistent with those in the EPA's ISC model.

Terrain Effects: The plume trajectory is modified by a simple "half-height" correction factor, in order to account for plume lifting by terrain during neutral and unstable conditions.

Limitations: Source emission rate should be fairly continuous, i.e. it should vary by less than a factor of two over 1-h period. Sources should have small enough apertures that they can be represented as point sources (e.g. smoke stacks). Because the turbulence parameterizations and the definitions of Lagrangian time scales in HPDM are most valid for the middle portion of the planetary boundary layer, the source heights that are modeled should not be less than about 50 m. Because the corrections in HPDM for the effects of terrain are most valid when the ratio of terrain height to stack height is much less than unity, the model is limited to terrain heights that are less than about one-half of the stack height.

3. METEOROLOGICAL PARAMETERIZATIONS

An operational model such as HPDM must be capable of producing accurate predictions for all hours of the year, including hours with precipitation, with snow cover, and with rapidly changing conditions. A model developer soon discovers that the standard references (e.g. Stull, 1988; Wyngaard, 1988) are able to provide reliable boundary-layer formulae for most but not all hours during a year. For example, while many researchers have studied the growth of the convective mixed layer in the morning, few have studied the gradual decay and then collapse of the mixed layer in the late afternoon. Also, most boundary-layer field experiments are shut down during rainy periods and during frontal passages.

The predictions of a model such as HPDM should be robust; i.e. they should not fluctuate wildly when an input parameter is varied by a slight amount. Furthermore, the variations of predictions should be continuous as input parameters vary (e.g. as atmospheric stability passes from slightly stable to slightly unstable).

Hanna and Chang (1992) present a complete description of recent improvements to the HPDM meteorological parameterizations, including comparisons with field observations. Emphasis is on predictions of the sensible heat flux, Q_H, the friction velocity, u_*, and turbulent energy components, σ_v and σ_w. It is found that the errors in the predictions of these parameters are about $\pm 20\%$ when the magnitudes of the parameters are large. However, when the magnitudes of these parameters are small (e.g.

*For further information, contact EPRI-ASDC, c/o Sigma Research Corporation, 196 Baker Avenue, Concord, MA 01742, U.S.A.

$\sigma_w < 0.2\ \mathrm{m\,s^{-1}}$) the errors in the predictions are as large as the mean values of the parameters.

Research on the use of boundary-layer formulae in dispersion models is fairly active, with ongoing studies by scientists such as Gryning *et al.* (1987) and Irwin and Paumier (1990). Our work draws upon the research of others and puts together a robust scheme which provides the required input parameters for the HPDM dispersion module.

3.1. *Surface heat flux Q_H and friction velocity* u_*

The HPDM meteorological parameterization scheme is based on proper specification of the sensible heat flux, Q_H, and the friction velocity, u_*. These parameters are occasionally observed as part of intensive research programs, using their definitions:

$$Q_H = c_p \rho \overline{w'T'} \tag{1}$$

$$u_* = (-\overline{u'w'})^{1/2}, \tag{2}$$

where u', w' and T' are turbulent fluctuations in horizontal wind speed, vertical wind speed and temperature, respectively. The parameter c_p is the specific heat of air at constant pressure, and ρ is the density of air. Parameters Q_H and u_* are used to define the Monin–Obukhov length, L, and the convective scaling velocity, w^*:

$$L = u_*^3 T \rho c_p / (0.4 g Q_H) \tag{3}$$

$$w_* = ((g Q_H / c_p \rho T) h)^{1/3} \quad \text{(valid only for } Q_H > 0\text{)}, \tag{4}$$

where T is absolute temperature, g is acceleration due to gravity, and h is mixing depth.

If the sensible heat flux, Q_H, is not observed, it can be estimated from the surface energy balance formula:

$$Q^* = Q_H + Q_E + Q_G, \tag{5}$$

where Q^* is the net radiation flux (including short- and longwave components), Q_E is the latent heat flux, and Q_G is the heat flux into the ground. We are ignoring the anthropogenic heat flux, which is highly variable and uncertain. It is assumed that $Q_G = aQ^*$, where $a = 0.1$ for rural areas and $a = 0.3$ for urban areas (Doll *et al.*, 1985).

The latent heat flux, Q_E, is parameterized using the approach suggested by Holtslag and van Ulden (1983), who define a surface moisture availability factor, α. HPDM assumes the following values for α as a function of land use:

- $\alpha = 0.0$–0.2 (dry desert with no rain for months)
- $\alpha = 0.2$–0.4 (arid rural area)
- $\alpha = 0.4$–0.6 (crops and fields, mid-summer during periods when rain has not fallen for several days)
- $\alpha = 0.5$–1.0 (urban environment, some parks)
- $\alpha = 0.8$–1.2 (crops, fields, and forests with sufficient soil moisture)
- $\alpha = 1.2$–1.4 (large lake or ocean with land more than 10 km distant).

With these definitions, equation (5) becomes:

$$Q_H = \left[\frac{(1-\alpha)+S}{1+S}\right] Q^*(1-\alpha) - \alpha\beta', \tag{6}$$

where β is a constant, assumed equal to $20\ \mathrm{W\,m^{-2}}$, that accounts for the fact that the sensible heat flux becomes negative before sunset. The parameter S is defined by $c_p/(L_e\,\mathrm{d}q_s/\mathrm{d}T)$, where L_e is the latent heat and $\mathrm{d}q_s/\mathrm{d}T$ is the slope of the saturation specific humidity curve (the Clausius–Clapeyron relation). The value of S varies with temperature, with a value of 2.01 at a temperature of -5 C and a value of 0.21 at a temperature of 35 C.

The net radiation, Q^*, is sometimes observed, but usually has to be parameterized based on albedo, A, solar elevation angle, ν, fractional cloud cover, N, shortwave radiation flux, Q_{sw}, and surface temperature, T:

$$Q^* = ((1-A)Q_{sw} + c_1 T^6 - \sigma T^4 + c_2 N)/(1+c_3), \tag{7}$$

where σ is the Stefan–Boltzmann constant, $5.67 \times 10^{-8}\ \mathrm{W\,m^{-2}\,K^{-4}}$, and the constants $c_1 = 5.31 \times 10^{-13}\ \mathrm{W\,m^{-2}\,K^{-6}}$ and $c_2 = 60\ \mathrm{W\,m^{-2}}$. The parameter c_3 is given by the formula:

$$c_3 = 0.38((1-\alpha)S + 1)/(S+1). \tag{8}$$

The albedo, A, for various land surfaces is found in several references. Hanna and Chang (1991) list values for several land types and seasons, as suggested for HPDM. If the shortwave radiation, Q_{sw}, is not observed, it can be parameterized as a function of solar elevation angle, ν, and fractional cloud cover, N (Holtslag and van Ulden, 1983):

$$Q_{sw} = ((990\ \mathrm{W\,m^{-2}})\sin\nu - 30\ \mathrm{W\,m^{-2}})(1 - 0.74\ N^{3.4}), \tag{9}$$

where the constants are derived for an agricultural site in the Netherlands and will be slightly different at another site.

The friction velocity, u_*, can be estimated using a knowledge of the sensible heat flux, Q_H, an observation of the wind speed, u, at a height, z, and the standard wind speed profile equation:

$$u = \frac{u_*}{0.4}\left(\ln\frac{(z-d)}{z_0} - \psi(z/L)\right), \tag{10}$$

where ψ is a universal dimensionless function (Stull, 1988). The surface roughness length, z_0, and the displacement length, d, can be estimated from the height of the roughness elements, h_r, using the approximate formulae $z_0 \sim 0.1\ h_r$ and $d \sim 0.5\ h_r$. Because ψ is a function of z/L and L is a function of u_*, a straightforward analytical solution for u_* is possible only for stable conditions, when $\psi(z/L) = -4.7z/L$. In that case, Weil and Brower (1983) derive the equation:

$$u_* = \frac{0.2u}{\ln((z-d)/z_0)} \times \left[1 + \left(1 - 4\left(\frac{4.7 g z \theta_* \ln((z-d)/z_0)}{0.4 T u^2}\right)\right)^{1/2}\right]. \tag{11}$$

A first estimate of the scaling temperature, θ_{*1}, can be made using Holtslag and van Ulden's (1983) empirical equation:

$$\theta_{*1}=0.09(1-0.5\,N^2), \tag{12a}$$

where θ_{*1} has units of K. In order to assure a real solution to equation (11), Weil and Brower (1983) set the following limit to θ_*:

$$\theta_{*2}=0.4\,Tu^2/(18.8\,gz\ln((z-d)/z_0)) \tag{12b}$$

and then assume that the correct θ_* is the smaller of θ_{*1} and θ_{*2}, with the additional condition that there is an absolute upper limit of 0.05 m K s^{-1} to the product $u_*\theta_*$ (i.e. the downward-directed sensible heat flux).

Because the function $\psi(z/L)$ is too complicated during unstable conditions to permit an analytical solution to equation (10) for u_*, HPDM uses an analytical approximation proposed by Wang and Chen (1980):

$$u_*=\frac{0.4u}{\ln[(z-d)/z_0]}[1+d_1\ln(1+d_2d_3)], \tag{13}$$

where

$$d_1=0.128+0.005\ln(z_0/(z-d)) \quad \text{if } z_0/(z-d)\leqslant 0.01$$
$$=0.107 \quad \text{if } z_0/(z-d)>0.01$$
$$d_2=1.95+32.6(z_0/(z-d))^{0.45}$$
$$d_3=\frac{Q_H}{\rho c_p}\frac{0.4g(z-d)}{T}\left(\frac{\ln((z-d)/z_0)}{0.4u}\right)^3.$$

The term $d_1\ln(1+d_2d_3)$ represents the correction due to instability.

The wind profile formula (equation 10) is, in principle, valid over any type of surface, ranging from ice flats to urban areas. Over rough surfaces such as forests or urban areas, observations show that, at night, the depth of the mechanically well-mixed layer is at least two or three times the height, h_r, of the roughness elements (Uno *et al.*, 1988). Because L is a measure of the depth of the mechanically well-mixed layer, then the calculated L should not be permitted to drop below about 3 h_r. The "minimum L" values used by HPDM are defined by the EPA/Auer (1978) land-use classification scheme as shown in the scheme below. These values are first estimates that can be refined as experience is gained.

3.2. *Profiles of turbulence components (σ_v and σ_w)*

The HPDM model, like other state-of-the-art models, assumes that the rate of growth of lateral and vertical dispersion is proportional to the lateral and vertical turbulence components, σ_v and σ_w, at the height of the plume. If observations of σ_v and σ_w are not available, it is necessary to parameterize them by empirical formulae based on analyses of observations at other sites. It is assumed that all parameters are averaged over 1 h.

Daytime.

$$\sigma_v=a_v(4.00u_*^2+0.35w_*^2)^{1/2}, \tag{14}$$

where the constant $a_v=1.0$ for $0<z/h\leqslant 1.0$ and $a_v=0.5$ for $z/h>1.0$.

Finally, $\sigma_v=\max(0.5\text{ m s}^{-1}, \sigma_v(\text{equation 14}))$. (15)

$$\sigma_w=u_*(1.44+2.9(-z/L)^{2/3})^{1/2} \text{ for } z/h\leqslant 0.1 \tag{16}$$

$$\sigma_w=a_w(1.44u_*^2+0.35w_*^2)^{1/2}, \tag{17}$$

where the constant $a_w=1.0$ for $0.1<z/h\leqslant 1.0$ and $a_w=0.5$ for $z/h>1.0$.

Equations (14), (16) and (17) are from Panofsky *et al.* (1977) and Hicks (1985). However, the assumptions that $a_v=0.5$ and $a_w=0.5$ at heights above the mixed layer ($z/h>1.0$) are highly arbitrary, since there are very few observations available at those heights. Equation (15) is based on the finding by many investigators (e.g. Hanna, 1986) that meandering has a strong effect on hourly averaged lateral turbulence, imposing a minimum value of σ_v of 0.5 m s^{-1}.

Nighttime.

$$\sigma_v=2.0u_*(1-0.5z/h), \quad z/h\leqslant 1.0 \tag{18a}$$

$$\sigma_v=u_*, \quad z/h>1.0. \tag{18b}$$

Finally, $\sigma_v=\max(0.5\text{ m s}^{-1}, \sigma_v$ (equation 18a or 18b)).

$$\sigma_w=1.2u_*(1-(1-a_w)z/(100\text{ m})), \quad z\leqslant 100\text{ m} \tag{19}$$

$$\sigma_w=1.2a_wu_*, \quad z>100\text{ m}, \tag{20}$$

where the constant $a_w=0.15$ for clear skies ($N<0.8$) and hours before and including 10 p.m. and $a_w=0.70$ for hours of 11 p.m. or later and any cloudy nighttime hour. An earlier version of HPDM used $a_w=0.15$ at heights above 100 m for all nighttime hours, but it was discovered that this assumption failed to account for

Scheme 1

Auer (1978) Land-use class	Description	Minimum L (m)
C1 (commercial)	>40-storey buildings	150
	10–40-storey buildings	100
	<10-storey building	50
I1 and I2 (industrial)		50
R3 (compact residential)		50
R1 and R2 (residential)		25
A (agricultural)		5

the nocturnal jet and for the turbulence that is present aloft during cloudy conditions. Because there are practically no field data at $z/h > 1.0$, it is probable that the value of the constant, a_w, will be changed as observations become available. Furthermore, it should be recognized that the assumption of 11 p.m. as the time of initiation of the nocturnal jet is valid only for mid-latitude summers, and may need to be modified for other latitudes and seasons.

3.3. *Profiles of temperature*

The potential temperature gradient, $d\theta/dz$, is needed for calculation of plume rise. If the stack height, h_s, is less than the mixing height, h, then $d\theta/dz$ is assumed to equal 0.0 during the daytime and is calculated from the following formula (from Businger *et al.*, 1971) during the nighttime:

$$d\theta/dz = (\theta_*/0.4h_s)[0.74 \ln((h_s-d)/z_0) + 4.7(h_s-d)/L], \quad (21)$$

where θ_* is obtained from equation (12). If $h_s \geq L$ during the nighttime, then L is substituted for h_s, recognizing the fact that equation (21) is valid only at $z/L < 1$.

If the stack height is greater than the mixing depth (i.e. $h_s/h > 1$), then $d\theta/dz$ at plume elevation is approximated by the following empirical formulae:

$$d\theta/dz = 0.005°C\,m^{-1} \quad \text{for } L < 0 \quad (22a)$$

$$d\theta/dz = 0.010°C\,m^{-1} \quad \text{for } L > 0. \quad (22b)$$

These default temperature gradients are similar to those in the EPA models, but are based on more recent observations at both rural and urban sites (see Hanna and Chang, 1991). Of course, if on-site observations are available, they should be used. But until remote sounders become routinely available, it will be necessary to use the empirical formulae given above.

3.4. *Mixing depth* h

Most of the formulae for wind, temperature and turbulence profiles given in this section require input of the mixing depth, h. Observations of mixing depth should be used if available and if there is expected to be little uncertainty. We caution the reader that some types of instruments, such as Doppler acoustic sounders, may produce unreliable estimates of mixing depth during many time periods, which can translate into erroneous predictions of ground-level concentrations. Parameterizations of temperature gradients and turbulent components by HPDM are different above and below the mixing depth, and, as will be seen in Section 4, several of the dispersion algorithms are strong functions of the mixing depth. For these reasons, it is better to err on the high side when estimating mixing depths from observations.

HPDM uses the following formulae for mixing depth:

Nighttime.

$$h = (L/3.8)(-1 + (1 + 2.28u_*/fL)^{1/2}). \quad (23)$$

This interpolation formula was suggested by Nieuwstadt (1981). The Coriolis parameter, f, equals roughly $10^{-4}\,s^{-1}$ at mid-latitudes. The solution approaches $0.3\,u_*/f$ during nearly neutral conditions and approaches $0.4\,(u_*/fL)^{1/2}$ during very stable conditions.

Daytime. Weil and Brower (1983) suggest a modification to Carson's (1973) prognostic formula, which requires knowledge of the early morning temperature profile and the time history of surface heat flux. This algorithm is described in Hanna and Chang (1991).

Neutral conditions. The mixing depth calculations for nighttime and daytime are replaced by the following calculation during neutral conditions (as defined by z_0 and L on Golder's, 1972, diagram):

$$h = 0.3u_*/f. \quad (24)$$

This value of h is usually relatively large (e.g. $h \sim 1500$ m when $u_* = 0.5\,m\,s^{-1}$), thus insuring that typical stack plumes are not significantly affected by the mixing depth when equation (24) is used.

3.5. *Limitations of boundary-layer parameterizations*

We have tried to point out the times and the locations where the above parameterizations are least well known and where additional observations and theoretical analyses are necessary. Errors are found to be largest during the following conditions:

- light winds ($u < 5\,m\,s^{-1}$) associated with weak net radiation ($Q^* < 100\,W\,m^{-2}$)
- late afternoon, when the boundary-layer is gradually collapsing
- periods when a nocturnal jet forms at elevations of 100–300 m
- any time when the mixing depth is below the stack height.

4. DISPERSION PARAMETERIZATIONS

HPDM uses four alternate types of dispersion parameterizations, depending on the magnitude of the stability parameter, L, and whether the plume elevation (after plume rise) is much less than, of the same order as, or much greater than the mixing depth. Interpolation formulae are used to prevent discontinuities in concentration predictions as input parameters are varied by a small amount. Approximate criteria for use of the four types of models are given in Fig. 1. The transition zones between the regions on Fig. 1 are determined by the magnitudes of the following dimensionless variables:

Dimensionless plume buoyancy flux.

Convective: $$F_* = F/uw_*^2 h, \quad (25a)$$

neutral: $$F_{*n} = F/uu_*^2 h, \quad (25b)$$

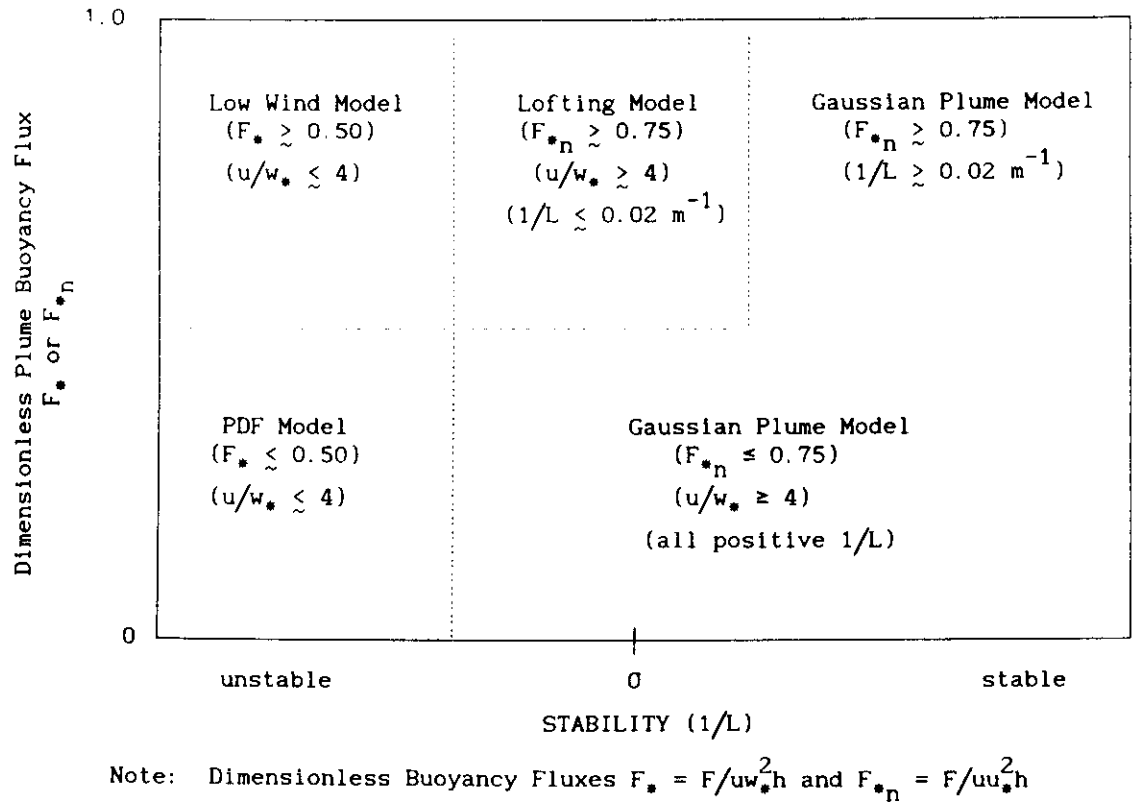

Fig. 1. Diagram of situations for which four alternate dispersion models in HPDM are valid; h is mixing depth, L is Monin–Obukhov length, w_* is convective scaling velocity and F is plume buoyancy flux. The dashed–dotted boundaries are only approximate, since u/w_* is not a one-to-one function of $1/L$, and F_* and F_{*n} are not one-to-one functions of $1/L$. The boundary between the lofting model and the Gaussian plume model is more precisely determined by Golder's (1972) nomogram, which yields the value of $1/L = 0.02$ m^{-1} in the above figure for $z_0 = 0.01$ m. In the HPDM model there are smooth transitions from one model to another as $1/L$, F_*, or F_{*n} change.

where the plume buoyancy flux is given by

$$F = (g/T) w_s R_s^2 \Delta T_s,$$

and w_s is stack plume exit speed, R_s is stack plume radius and ΔT_s is initial stack plume temperature excess. The plume begins to interact with the mixing lid when $F_* \sim 0.1$ or $F_{*n} \sim 0.5$, and full interaction occurs when $F_* \sim 0.5$ or $F_{*n} \sim 0.75$.

Convective stability parameter. A value of $u/w_* \sim 4$ marks the transition point between a boundary layer dominated by mechanical and convective turbulence (Weil, 1988).

Golder (1972) nomogram function for value of L that separates neutral from stable conditions. Golder (1972) presents a diagram in which the dividing line between neutral and stable conditions is given as a function of roughness length, z_0, and Monin–Obukhov length, L. For a flat grassy surface with $z_0 \sim 0.01$ m, this dividing line occurs at a value of L of about 50 m. For each order of magnitude increase in z_0 the dividing value of L increases by about a factor of two.

Details of the four alternate models for dispersion are given in the next few sections. Prior to application of these dispersion models, the plume rise is calculated using Briggs' (1975) formulae, which are not described here because they are in wide use in other models and because they were thoroughly discussed by Hanna and Paine (1989).

In addition, HPDM now accounts for the effects of terrain using methods similar to those in EPA's MPTER model. A so-called "half-height" correction factor is applied to the plume elevation above ground level, h_e, during neutral and unstable conditions. This correction is valid only for receptor heights less than about one-half of the stack height, and is discussed in detail in the user's guide (Hanna and Chang, 1991).

4.1. *Gaussian plume model*

The so-called "Gaussian plume model" is used by HPDM for stable conditions. It is also used for neutral conditions when the plume elevation is much less than the mixing height (i.e. when $F_{*n} = \leqslant 0.75$):

$$\begin{aligned} C = {} & (Q/(2\pi u \sigma_y \sigma_z)) \exp(-0.5((y-y_p)/\sigma_y)^2) \\ & \times (\exp(-0.5((z-h_e)/\sigma_z)^2) \\ & + \exp(-0.5((z+h_e)/\sigma_z)^2)) \\ & + \text{secondary reflection terms}, \end{aligned} \tag{26}$$

where C is concentration in mass per unit volume, Q is source emission rate in mass per unit time, and u is wind speed at a height equal to 0.5 times the stack height. The parameters y and z are lateral and vertical position, y_p is lateral position of the plume centerline, and σ_y and σ_z are lateral and vertical plume dispersion parameters.

In case building downwash occurs, HPDM contains algorithms so that the values of σ_y and σ_z approach those used in the EPA's ISC model. When building downwash is not an issue (i.e. when the stack height is at least 2.5 times the building height), the following formulae are used for σ_y and σ_z:

$$\sigma_y^2 = \sigma_{yt}^2 + \sigma_{yb}^2 \quad (27)$$

$$\sigma_z^2 = \sigma_{zt}^2 + \sigma_{zb}^2, \quad (28)$$

where subscript b indicates dispersion induced by buoyant plume rise. This component is given by (Pasquill, 1976):

$$\sigma_{yb}^2 = \sigma_{zb}^2 = (\Delta h^2/12.25), \quad (29)$$

where Δh is the plume rise at downwind distance, x. Subscript t indicates the atmospheric turbulence-induced dispersion, which is assumed to be a function of the local turbulence components:

$$\sigma_{yt} = \sigma_v (x/u)[1 + 0.9(x/u\ 15000\,\mathrm{s})^{1/2}]^{-1} \quad (30)$$

$$\sigma_{zt} = \sigma_w (x/u)[1 + x/(2uT_{Lz})]^{-1/2}. \quad (31)$$

The turbulence components σ_v and σ_w may be observed on site, or may be parameterized using equations in Section 3.2.

The vertical Lagrangian time scale, T_{Lz}, represents the effective eddy sizes that act on the plume as it disperses between the source and the downwind receptor position of interest, x. For elevated sources ($h_e \gtrsim 50$ m), this time scale can be represented by its value at the height h_e. However, for near-ground level sources ($h_e < 10$ m), as the plume diffuses vertically and it is influenced by larger and larger eddy scales, the effective time scale will become larger than that appropriate for the height h_e. For this reason, the following formulae are valid only for elevated sources ($h_e \gtrsim 50$ m).

During stable conditions, the Lagrangian time scale, T_{Lz}, can be assumed to be a function of Monin–Obukhov length, L, vertical potential temperature gradient, $d\theta/dz$, and plume height, h_e:

$$\text{if } h_e \leqslant L, \qquad T_{Lz} = 2h_e/\sigma_w \quad (32)$$

$$\text{if } L \leqslant 10\text{ m}, \qquad T_{Lz} = 0.54/s^{1/2} \quad (33)$$

$$\text{if } 10\text{ m} < L < h_e, \quad T_{Lz} = (2h_e/\sigma_w)(L-10)/(h_e-10) + (0.54/s^{1/2})(h_e - L)/(h_e - 10), \quad (34)$$

where L and h_e must be expressed in meters in interpolation formula (34). The stability parameter, s, defined by $[(g/T)(d\theta/dz)]$, is the square of the so-called Brunt–Vaisala frequency.

For unstable conditions ($L < 0$), T_{Lz} can be assumed to be a function of Monin–Obukhov length L, plume height, h_e, mixing depth, h, and stability parameter, s:

$$\text{if } h_e \leqslant |L|, \qquad T_{Lz} = 0.4h_e/[\sigma_w(0.55 - 0.38h_e/|L|)] \quad (35)$$

$$\text{if } |L| < h_e \leqslant h, \quad T_{Lz} = (0.6h/\sigma_w) \times (1 - \exp(-5h_e/h) - 0.0003\exp(8h_e/h)) \quad (36)$$

$$\text{if } h_e > h, \quad T_{Lz} = 0.54/[s]^{1/2}, \quad (37)$$

where the potential temperature gradient, $d\theta/dz$, in the capping inversion is either the observed value or the parameterized value of 0.005 °C m^{-1}.

Note that it is implied in equation (30) that T_{Ly} is assumed to be a constant, 15,000 s, for all conditions, based on the analysis of stack plume σ_y data described by Hanna (1986) and the analysis of Indianapolis σ_y observations reported in Hanna and Chang (1991). The T_{Lz} formulae for stable conditions are slight modifications of Hunt's (1982) suggestions and the T_{Lz} formulae for unstable conditions are based on Caughey's (1982) results.

4.2. *PDF model*

The probability density function (PDF) model of Weil and Brower (1984) is used during convective conditions ($u/w^* < 4$) when the plume remains well below the mixing lid ($F_* < 0.5$) and when the plume elevation exceeds about 0.1 h. This model, whose details are described by Hanna and Paine (1989), accounts for the differences in the turbulence characteristics of updrafts and downdrafts in the convective boundary layer. It is called the PDF model because it specifies the bimodal pdf of the vertical velocity distribution during convective conditions. The vertical velocity pdf is fairly constant at heights between about $0.1h$ and h. The ensemble-averaged crosswind ground-level (i.e. $z = 0$) concentration, $C^y = \int_{-\infty}^{\infty} C\,dy$, nondimensionalized by Q/uh, is found to be

$$\frac{C^y uh}{Q} = \frac{1.2}{\sqrt{2\pi}\sigma_{z1}^*}\exp\left[\frac{-h_1^{*2}}{2\sigma_{z1}^{*2}}\right] + \frac{0.8}{\sqrt{2\pi}\sigma_{z2}^*}\exp\left[\frac{-h_2^{*2}}{2\sigma_{z2}^{*2}}\right], \quad (38)$$

where the first term represents turbulent diffusion in downdrafts and the second term represents turbulent diffusion in updrafts, and

$$\sigma_{zi}^* = (0.64F_*^{2/3}X_*^{4/3} + b_i^2 X_*^2)^{1/2}$$

$$h_1^* = h_s^* + 1.6F_*^{1/3}X_*^{2/3} + a_i X_*$$

$$h_s^* = \frac{h_s}{h}, \quad F_* = \frac{F}{uw_*^2 h}, \quad X_* = \frac{w_* x}{uh} \quad \text{and} \quad (39)$$

$i = 1$ or 2, $a_1 = -0.35$, $a_2 = 0.4$, $b_1 = 0.24$, and $b_2 = 0.48$. An image source, at $z = -h_s$, is assumed in equation (38). In the HPDM model, other image sources at $z = -2h - h_s$, $4h + h_s$, etc. are assumed in order to conserve mass and satisfy the no-flux condition at the ground and at the mixing lid.

To calculate point concentrations, the following formulae are used in the PDF model:

$$C = (C^y/\sqrt{2\pi}\sigma_y)\exp(-(y - y_p)^2/2\sigma_y^2) \quad (40)$$

$$\sigma_y = (\sigma_v x/u)/(1 + 0.5x/(uT_{Ly}))^{1/2} \quad \text{if } F_* < 0.1 \quad (41)$$

$$\sigma_y = 1.6F_*^{1/3}X_*^{2/3}h \quad \text{if } F_* > 0.1 \text{ and } u/w_* \geqslant 2 \quad (42a)$$

$$\sigma_y = 0.8F_*^{1/3}X_*^{2/3}h \quad \text{if } F_* > 0.1 \text{ and } u/w_* < 2, \quad (42b)$$

$$\text{where } T_{Ly} = 1.1\sigma_v/\varepsilon \quad (43)$$

and the eddy dissipation rate, ε, is given by

$$\varepsilon=(0.5w_*^3/h)+(u_*^3/0.4(h-h_s))\ln(h/h_s). \quad (44)$$

4.3. *Low-wind convective scaling model*

When the plume rises up near the top of the mixed layer (i.e. $F_* \geq 0.5$) during convective conditions (i.e. $u/w_* \leq 4$), HPDM makes use of the low-wind convective scaling model proposed by Hanna and Paine (1987). The model is based on an analysis by Briggs (1985) of several sets of field and laboratory data. The specific formulae that are used for ground-level concentration, C, are listed below:

$$C=(0.021Qw_*^3x^{1/3}/(F^{4/3}h))\exp(-0.5(y-y_0)^2/\sigma_y^2) \quad (45)$$

for $x<10F/w_*^3$, where σ_y is defined by equation (42b).

$$C=((Q/(w_*xh))\exp(-7F/(xw_*^3)^{3/2}) \times \exp(-0.5(y-y_0)^2/\sigma_y^2) \quad (46)$$

for $x \geq 10F/w_*^3$, where $\sigma_y=0.6x_*h$.

These equations can be used to derive a formula for the maximum ground-level concentration for any particular hour:

$$C_{max}=0.04Qw_*^2/F. \quad (47)$$

Because the ratio of mass emission rate to buoyancy flux, Q/F, is likely to remain nearly constant at a given site, it is seen from equation (47) that the maximum concentration is directly proportional to the turbulent energy, w_*^2, and inversely proportional to the mixing depth, h. Note that the wind speed does not appear in this formula, verifying the original assumption that turbulence and dispersion processes in the strongly convective boundary-layer are independent of the wind speed.

4.4. *Lofting model for neutral conditions*

The lofting model, originally proposed for convective conditions by Weil and Corio (1988), has been modified by Weil (1991) so that it is applicable to both neutral and convective conditions. It accounts for the situation where a plume rises up to the top of the mixed layer, impinges against the mixing cap, and spreads horizontally. Mixing to the ground is delayed until the upward velocities due to the plume buoyancy die away sufficiently that they are overwhelmed by ambient turbulence. The ratio of these two effective velocities (internal plume and ambient) is defined by the dimensionless function, ϕ:

$$\phi=0.8(F/x)^{1/3}/\sigma_w, \quad (48)$$

where the constant, 0.8, has been calibrated with limited field data and should be further refined using data from a wide variety of sites.

Because this model and the low-wind model (described in the previous section) would often apply to the same hours during convective conditions, HPDM currently uses the low-wind model during convective conditions. The low wind model has been more carefully tested with field data than the lofting model. However, HPDM does use the lofting model for neutral conditions, as pictured by the schematic diagram in Fig. 1 and as defined by the following criterion:

$$F_{*n}=F/uu_*^2h>0.75,$$

with the condition that $u/w_*>4$ during unstable hours. During stable hours, the ratio $1/L$ should be less than a limit determined from the Golder (1972) nomogram (approximately equal to 0.02 m^{-1} when $z_0=0.01$ m).

Our experience shows that these criteria were satisfied during the Indianapolis tracer study (described in the next section) during cloudy periods when mixing depths were about 300–500 m all day. Such low mixing depths are generally imposed by synoptic conditions (e.g. a warm front in the vicinity).

The ground-level concentrations are given by

$$C=(Q/(\sqrt{2\pi}h\sigma_y u))(1-\text{erf}(\phi))\exp(-(y-y_p)^2/2\sigma_y^2), \quad (49)$$

where σ_y is given by:

$$\sigma_y=1.6F^{1/3}x^{2/3}u^{-1}. \quad (50)$$

5. EVALUATION OF HPDM WITH FIELD DATA

HPDM was previously evaluated with several hundred hours of SF_6 tracer data from rural power plants in Kincaid and Bull Run (Hanna and Paine, 1989). The new version of HPDM (Version 4.2) has been more extensively tested with independent SF_6 tracer data from an urban power-plant in Indianapolis and with 1 year of independent hourly SO_2 data from a rural power plant in Baldwin and an industrial region in Summit County. The characteristics of the three data sets are listed in Table 1, and diagrams of the monitoring networks at the three sites are given in Figs 2–4.

It is important to note that, for any application exercise at an existing industrial site, the conditions are not ideal. The surrounding terrain at each site mentioned above is reasonably homogeneous but there are often complications due to water bodies, buildings or hills. The on-site meteorological towers are not always in representative locations. The Summit County exercise was further impacted by the fact that the meteorological data that were used were from both an airport and a TV tower, which were located about 30 km apart, and the sources and receptors were scattered about the county at distances up to 20 km from either of the sources of meteorological data (see Fig. 4). Nevertheless, these data represent typical real-world source scenarios, and the results should be useful as part of a comprehensive model evaluation exercise.

In order to demonstrate the differences between the predictions of HPDM and the predictions of the

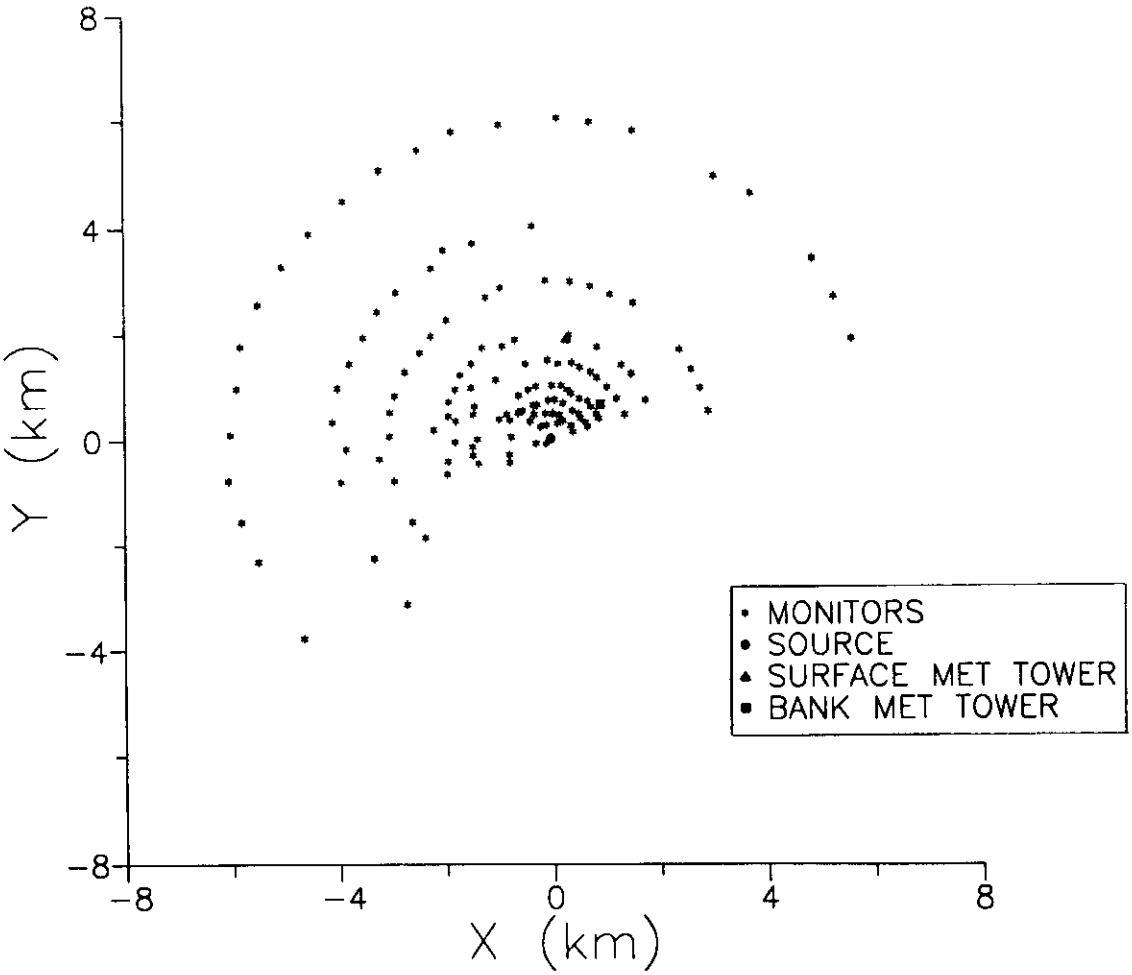

Fig. 2. SF_6 monitoring network in Indianapolis for 16 September 1985 field study. Positions of the power-plant source and the two meteorological towers are also shown.

models currently in use by the EPA, the appropriate EPA model was also applied to each site (RAM at Indianapolis, and ISC at Baldwin and Summit County).

The values of input parameters used by the HPDM model are given in Table 2. The roughness length varies with season at the Baldwin site, which is surrounded by farmland. The albedo varies with season at the Baldwin and Summit County sites. Because the Summit County site is a conglomeration of urban, suburban and industrial land-use, it is assumed to have a constant moderate roughness length of 0.1 m and a minimum L of 25 m. The moisture availability factor is assumed to be 0.5 at the drier Indianapolis urban site, 1.0 at the more moist Baldwin agricultural site (where there are also several lakes in the vicinity) and 0.8 at the intermediate Summit County site. Generally, the dilution wind speed is estimated using data from the top level of an on-site tower, and the wind speed used for calculating surface fluxes is taken from the 6–10 m level of a tower in an open area. The mixing depths were observed by a special on-site radiosonde program at Indianapolis, but were calculated by the HPDM model at Baldwin and Summit County using the morning radiosonde temperature profile from the nearest NWS station, along with the on-site calculated surface heat and momentum fluxes.

The EPA's RAM and ISC models do not make use of most of the input data used by HPDM in Table 2. The RAM and ISC models do require a wind speed which is assumed to be the 94 m bank tower wind observation at Indianapolis, the 100 m tower wind observation at Baldwin, and the 73 m tower observation at Summit County. The EPA models also require input of the mixing depth, and we use the same values used as input to HPDM. The EPA models in addition require input of the Pasquill–Gifford–Turner stability class, which is obtained by standard EPA procedures based on solar elevation angle, cloudiness and the wind speed from the level used for the surface flux calculations.

5.1. *Model performance measures and statistical procedures*

The HPDM and RAM or ISC models were applied to all hours of data from each site, producing 89 h of predictions of ground-level concentrations, C_p, at Indianapolis and 8760 h (i.e. 1 year) of predictions at Baldwin and Summit County. Predictions were made at all monitoring positions at each site. The hourly

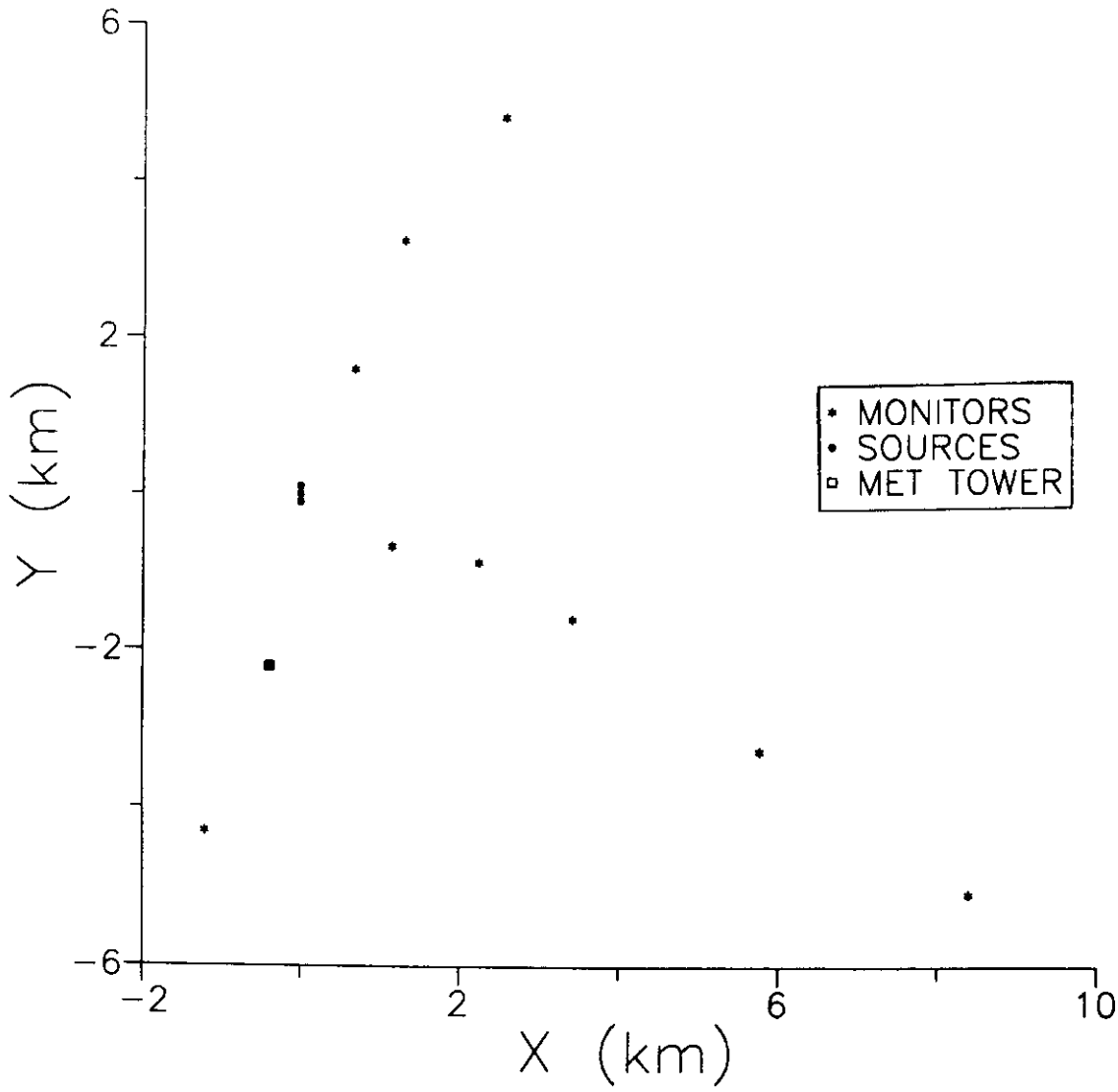

Fig. 3. SO_2 monitoring network at Baldwin. Positions of the three stack sources and the meteorological tower are also shown.

averaged SO_2 concentration predictions were combined into 3- and 24-h averages at Baldwin and Summit County, since the National Ambient Air Quality Standards (NAAQS) emphasize those averaging times. In the statistical comparisons, the maximum concentration anywhere on the monitoring arc is selected for a given time period. Thus it is highly likely that, for any time period, the observed and predicted maximum concentration, C_0 and C_p, will occur at different monitoring positions.

Because the NAAQS is keyed to the second-highest concentration, tables of those figures are included as part of our model evaluation. We also include several statistical performance measures that indicate the model performance over the entire data set (Hanna, 1989). In this paper, the following statistics are given:

$\mathrm{FB}=2(\overline{C_0}-\overline{C_p})/(\overline{C_0}+\overline{C_p})$: fractional bias, or relative difference in mean values,

FAC2: fraction of predictions that are within a factor of two of observations,

R: correlation coefficient between predicted and observed concentrations.

Confidence limits on differences in the statistics between the two models are calculated using resampling methods in order to determine if the differences are significant at the 95% confidence level.

In addition, model residuals (expressed as C_p/C_0) are plotted as a function of input meteorological parameters (such as u or L), in order to determine if the model has problems with over- or underpredictions during certain conditions. Based on the results of prior model evaluation exercises, it is expected that any set of C_p/C_0 values would show a scatter of $\pm 50\%$ or more, but it is hoped that the median C_p/C_0 values would show no trends as the input parameters vary. If there are trends in the residual plots, then it can be concluded that the scientific components of the model have not been properly formulated.

Table 1. Characteristics of three sites used for model evaluation

Site name	Sources	Hours of air quality data	Number of monitors (distances from source)	Meteorological data	Surrounding terrain
Indianapolis Perry K	one 83-m stack	89 h of SF_6 tracer data	about 160 (0.25–12 km)	on-site tower (10 and 93 m)	flat urban area
Baldwin	three 183-m adjacent stacks	8760 h of SO_2 data	10 (1.3–9.8 km)	on-site tower (10 and 100 m)	flat farmland, some lakes nearby
Summit County	20 stacks, all less than 100 m	8760 h of SO_2 data	12 (scattered over county)	airport plus TV tower (73 m)	rolling small urban/industrial/ residential region

Table 2. Input meteorological parameters used by models

Site	Roughness z_0 (m)	Albedo A	Moisture availability α	Wind speed for dilution	Wind speed for surface fluxes	Lateral turbulence input	Mixing depth input	Minimum L (m)
Indianapolis	1	0.18	0.5	94-m bank tower	10-m urban	10-m urban tower	Observed by on-site radiosonde	50
Baldwin	0.01–0.19	0.14–0.58	1.0	100-m tower	10-m tower	Not available	HPDM calculation using Salem radiosonde	2
Summit County	0.1	0.14–0.39	0.8	73-m tower	6-m from Akron airport	Not available	HPDM calculation using Pittsburgh radiosonde	25

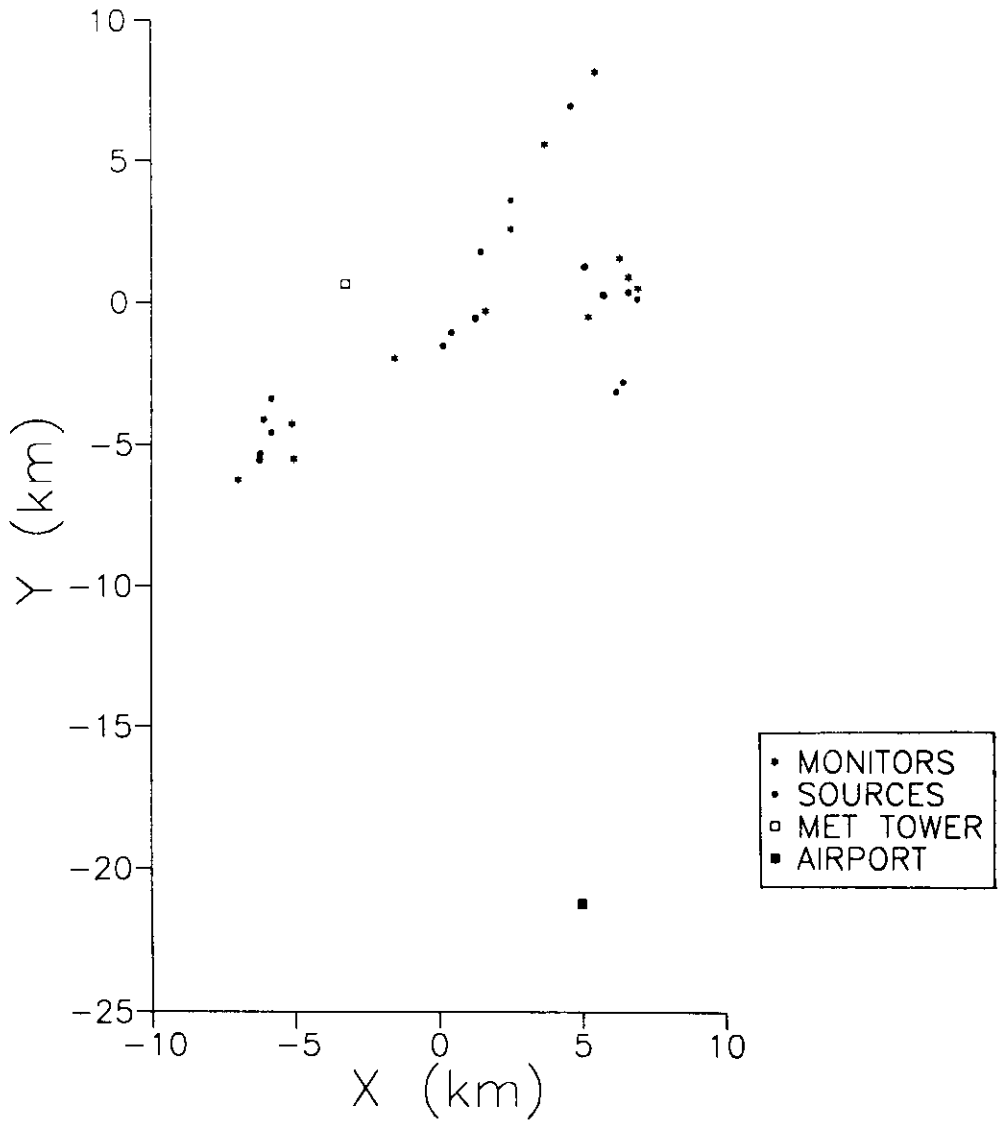

Fig. 4. SO_2 monitoring network at Summit County. Positions of the major SO_2 sources, the meteorological tower and the airport are also shown.

5.2. *Results of HPDM and RAM model evaluations at Indianapolis*

A total of 168 h of SF_6 tracer data were taken during 19 separate 8 or 9 h periods around the Perry K power plant in Indianapolis. The layout of the monitoring network for one of the experimental periods is given in Fig. 2. It is seen that the network of about 150 monitors is much denser than the network at the other two sites (Figs 3 and 4). The reason for the difference is that the Indianapolis study was an intensive research program, whereas the Baldwin and Summit County studies were routine SO_2 monitoring programs. Nine of the experimental periods at Indianapolis were used for initial analysis and model development, and 10 of the periods (accounting for 89 h) were reserved for final "independent" model testing. The results in this section pertain to those 89 h, which cover a wide range of times of the day and meteorological conditions (Hanna and Chang, 1991). To simplify the comparisons, the concentrations have been normalized by the SF_6 tracer gas emission rate (i.e. C_p/Q and C_0/Q).

Because there are only 89 h of data, it is possible to plot the predicted and observed normalized concentrations for each of the 10 test periods on one page, in order to "see" how well the model is performing. Figure 5 contains these 10 time series, showing that the HPDM predictions track the observations fairly well, although there are often differences of plus or minus a factor of two. Furthermore, on some days (such as 27–28 and 30 September and 3 October) there is a consistent bias towards under- or overpredictions during the entire test period.

The results of the statistical evaluation exercise at Indianapolis are summarized in Table 3. HPDM slightly overpredicts (by about 10%) the second-highest normalized concentration, whereas the RAM model overpredicts this value by over 50%.

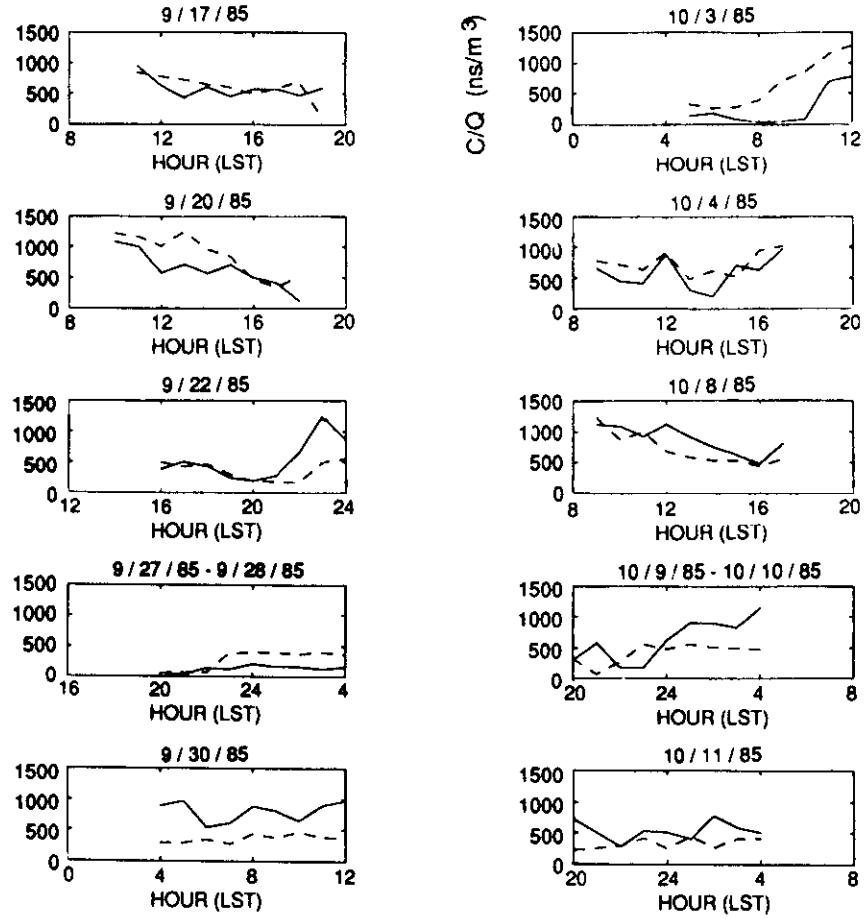

Fig 5. Observations (solid lines) and predictions (dashed lines) of C/Q (10^{-9} $\mu s\,m^{-3}$) for HPDM, for each hour of each period in the Indianapolis data set; C/Q represents the maximum value independent of position on the monitoring network.

Table 3. Performance measures for HPDM and RAM models for the evaluation data set (89 h) at Indianapolis. Normalized concentrations, C/Q, in units of $\mu s\,m^{-3}$ are used. FAC2 is the fraction of predictions within a factor of two of observations, and fractional bias, $FB = 2(\overline{C_o/Q} - \overline{C_p/Q})/(\overline{C_o/Q} + \overline{C_p/Q})$

	Second-highest C/Q	$\overline{C/Q}$	Correlation R	FAC2	FB
Observed	1135	558	–	–	–
HPDM	1255	532	0.44	0.66	0.05
RAM	1735	644	−0.24	0.62	−0.014

Both model predictions are fairly close to the overall average, with HPDM being 5% low and RAM being 14% high. There is a significant difference in the correlation coefficients, R, for the two models, since the RAM predictions are negatively correlated with the observations. The fraction of the predictions that are within a factor of two of the observations, FAC2, is similar for the two models (0.66 for HPDM and 0.62 for RAM).

Residual plots of C_p/C_0 for HPDM as a function of wind speed, stability index, height and hour of day are plotted in Fig. 6. The distributions of the N points in each category are represented as box plots in the figure. It is seen that there is a slight tendency to overpredict by about a factor of two at the lowest wind speed category and the lowest mixing height category. However, there are no major trends extending across two or three or more categories in these plots, suggesting that HPDM has no major problems in its underlying scientific formulations.

Residual plots for the distance, x, from the stack to the position of the ground-level maximum concentration for each hour are also of interest in a model evaluation exercise. Figure 7 contains residual plots of x_p/x_0 for HPDM for Indianapolis, following the same format as Fig. 6. There is evidence for a factor of two

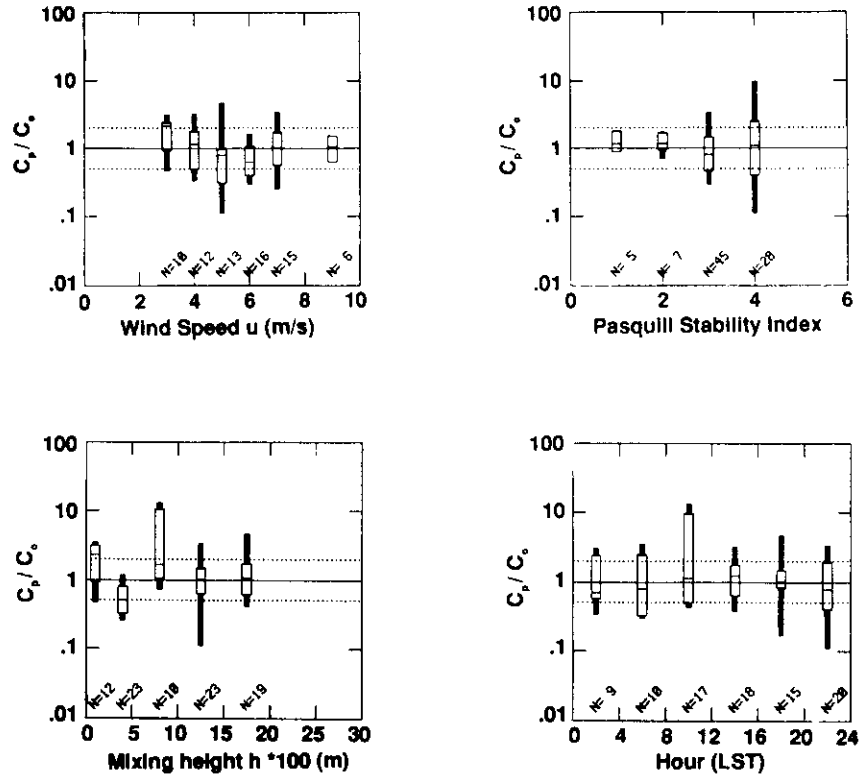

Fig. 6. Residuals of concentration predictions (C_p/C_0) plotted as a function of wind speed, stability index, mixing height and hour of day, for HPDM for 89 h in the evaluation data set at Indianapolis. Significant points on each box plot represent the average, the average ± one standard deviation, and the average ± two standard deviations. N is the number of points in each box.

overprediction of this distance at the lowest wind speed category and the lowest mixing height category. There is a clear trend with stability index, where underpredictions by about a factor of two of the distance to the maximum occur during unstable conditions and overpredictions during stable conditions. However, there are relatively few points ($N = 5$) in the unstable category. These results suggest that some more work may be necessary in order to improve the ability of HPDM to place the maximum concentration at the proper downwind distance. However, in order to derive and test improved formulae properly it is necessary to have extensive experimental data available from large monitoring networks (i.e. more than 100 monitors). Because such experimental programs cost millions of dollars it is unlikely that the required new data sets will become available soon.

5.3. *Results of HPDM and ISC model evaluations at Baldwin and Summit County*

The model applications at Baldwin and Summit County represent typical model exercises required by agencies as part of air permitting procedures. An entire year of hourly data is used, including some meteorological conditions not considered by the research scientists who originally developed the boundary-layer formulae that are used in the models. There are several stacks at each site, and the on-site meteorological observations and the SO_2 monitoring networks are limited (see Figs 3 and 4). Nevertheless, in order for HPDM to be accepted for general use, it must demonstrate its ability to simulate satisfactorily observed concentrations at sites such as these. Tables 1 and 2 contain information on the sites, the sources and the input meteorological data. The required tables of input meteorological data and source emissions data for the 8760 h at each site were prepared by ENSR Inc. under separate contract. Surface fluxes were calculated using data from the 10 m level of the meteorological tower at Baldwin, and using airport wind observations (at a height of 6 m) at Summit County. The wind speeds used to calculate plume rise and dilution were based on observations from the upper level (73–100 m) of the meteorological tower at both sites. The mixing depth was calculated by the HPDM model at both sites using radiosonde temperature profiles from the closest NWS upper-air station and using calculated on-site surface heat fluxes.

Table 4 contains statistics concerning the observed and predicted SO_2 concentrations (in $\mu g\,m^{-3}$) for three averaging times (1, 3 and 24 h) at the two sites. The annual averages are also given. The concentration observations are not normalized by the SO_2 source emission observations, Q, at Baldwin and Summit County because occasionally Q became very

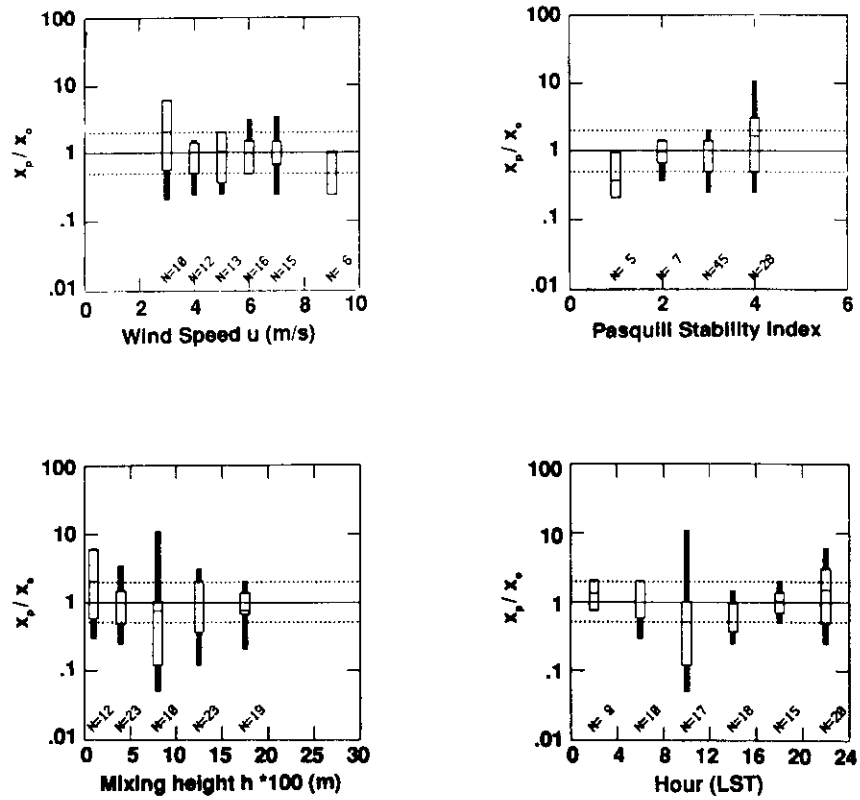

Fig. 7. Residuals of predicted distance to maximum concentration (x_p/x_0) plotted as a function of wind speed, stability index, mixing height and hour of day, for HPDM for the evaluation data set at Indianapolis. Significant points on each box plot represent the average, the average ± one standard deviation, and the average ± two standard deviations. N is the number of points in each box.

Table 4. Performance measures for HPDM and ISC models for the data sets at Baldwin and Summit County. The observed and predicted concentrations represent the maximum value at any monitoring location for each time period. The units of all SO_2 concentrations are $\mu g\,m^{-3}$. An asterisk indicates the better model in a particular group

Site and averaging time	C_{2ndHi}			Correlation R		Fraction within a factor of 2 (FAC2)	
	Obs.	HPDM	ISC	HPDM	ISC	HPDM	ISC
Baldwin							
1 h	1990	1975*	1933	0.42*	0.24	0.14*	0.03
3 h	960	1080*	690	0.51*	0.31	0.16*	0.05
24 h	200	220*	150	0.53*	0.33	0.38*	0.12
Annual	44	46*	11	—	—	—	—
Summit County							
1 h	1100	1750	1390*	0.38*	0.36	0.53*	0.49
3 h	1010	1120*	760	0.45*	0.45*	0.61*	0.61*
24 h	395	365*	285	0.52	0.61*	0.82*	0.74
Annual	163	203	153*	—	—	—	—

small during periods of plant start-up or shut-down at Baldwin, and because there were 20 independent sources in Summit County. It should be recalled that the observed and predicted concentrations that are analysed for each hour represent the maximum hourly averaged value at any of the monitor locations at that site (i.e. the locations of the observed and predicted maxima are usually different).

Asterisks are placed in Table 4 next to the best-performing model for a particular category. It is seen

that, for most of the C_{2ndHi} data, the asterisk is next to the prediction of the HPDM model. The main exception to this rule is seen in the Summit County data set, where the performance of the ISC model is better at the 1-h averaging time and the annual averaging time. The two sites can be considered to represent separate types of source scenarios. The data set from Baldwin represents isolated tall stacks, while the data set from Summit County represents a regional complex of many individual sources. At the Baldwin site, the HPDM model predictions of C_{2ndHi} are close (within about 10%) to the observations, while the ISC model consistently underpredicts by about 25–30%. Our analyses of the ISC model predictions suggest that the primary cause of these underpredictions is the tendency of the ISC model to underestimate vertical dispersion during nearly neutral conditions, leading to underestimates of ground-level concentrations for elevated sources. Because of the relatively small number of monitors (resulting in zero predictions at the monitor locations during about 50% of the hours in a year) and the effects of stochastic fluctuations, only about 14% of the hourly HPDM predicted concentrations are within a factor of two of the observations. For the same reasons, the correlation coefficient is only about 0.4 to 0.5. However, despite these mediocre values of the "factor of two" (FAC2) and correlation (R) statistics for HPDM, they are still significantly better than the corresponding ISC model predictions at the Baldwin site.

The HPDM model predictions are generally slightly better than the ISC model predictions at the Summit County site, although the differences are not usually significant. We believe that the variability in model performance at the Summit County site is primarily affected by the fact that the two meteorological sites were separated by 10–30 km from the sources, from the SO_2 monitoring sites, and from each other (see Fig. 4). The relatively high values (0.5–0.8) for the fraction of predictions that are within a factor of two of observations at the Summit County monitoring network are due to the regional aspect of the site, i.e. there are nearly always significant nonzero observations and predictions at some monitoring location. In contrast, at the Baldwin site (see Fig. 3), which is located in a rural area with only one large source of SO_2 in the region, a large fraction of the hours during the year were marked by nearly zero predictions or observations of concentrations, and hence the fraction within a factor of two was relatively low.

Our confidence in a model is increased if the meteorological conditions associated with its highest five predicted concentrations agree with those conditions associated with the highest five observed concentrations. This concept is tested in Table 5, where the median values of wind speed, u, mixing depth, h, and Monin–Obukhov length, L, for the highest five hourly observed and predicted concentrations are listed for the Baldwin and Summit County sites. It is seen that at the Baldwin site, both models are able to simulate the fact that the highest five observed concentrations occur during light-wind unstable conditions with moderate mixing depths. There are some minor differences, but they do not alter this general result. At the Summit County site, neither model is able to reproduce the precise range of meteorological conditions associated with the highest five observed concentrations, which occur during nighttime periods with moderately high winds and high mixing depths. Although the HPDM model concentration predictions are associated with more moderate wind speeds and lower mixing depths than observed, the model is able to reproduce the fact that the highest five concentrations occur at night. The ISC model, on the other hand, predicts the highest concentrations to occur during the day.

6. CONCLUSIONS AND RECOMMENDATIONS

The most recent version of the Hybrid Plume Dispersion Model (HPDM-Version 4.2) contains improved algorithms for estimating key boundary-layer parameters based on routine observations of wind speed and cloudiness. The model is also capable of assimilating detailed boundary-layer observations of turbulent velocities. The HPDM model contains state-of-the-art formulae for calculating dispersion in stable, neutral and convective conditions and for simulating plume interactions with the capping inversion at the top of the mixed layer. It can be applied to point source releases at any height above about 50 m over any type of surface, and it is limited to topographic situations where the height of the terrain is less than about one-half of the stack height.

An earlier version (3.0) of the HPDM model was evaluated by Hanna and Paine (1989) using hundreds of hours of tracer data obtained during special research studies at power plants in relatively flat rural terrain. The objective of this new study was to evaluate the improved version of the model (HPDM-4.2) in an urban setting in which high-quality tracer data were available, and in typical EPA regulatory settings in which 1 year of routine hourly data are available.

Table 5. Median meteorological conditions (wind speed, u, mixing depth, h, and Monin-Obukhov length, L) associated with the highest five hourly observed and predicted concentrations at two sites

Site and parameter	Observed	HPDM	ISC
Baldwin			
u (m s^{-1})	1.7	2.6	3.3
h (m)	680	370	1000
L (m)	−9	−8	−10
Summit County			
u (m s^{-1})	11	4.5	3.1
h (m)	2500	170	190
L (m)	700	70	−25

The urban site was an 83 m power-plant stack in Indianapolis. The two routine sites that were chosen were the Baldwin power plant (three 183-m stacks, surrounded by 10 SO_2 monitors) and the Summit County industrial region (20 stacks and 12 monitors scattered around the county). For comparison purposes, the EPA's RAM and ISC models were also included in the model evaluation exercises. Emphasis was on the highest predicted and observed concentration during a given hour at any monitoring position on the network.

The following conclusions can be made:

- The HPDM model is a significant improvement over the RAM model at the Indianapolis site, where HPDM's C_{2ndHi} prediction is within 5% of the observation.
- The HPDM predictions of the "second-highest" concentration for 1-, 3- and 24-h averaging times are very close (within 13%) to the observations at the Baldwin site. The ISC model tends to underpredict by about 25% at that site.
- The HPDM predictions of the "second-highest" concentration at the Summit County site are close (within 17%) to the observations for the 3- and 24-h averaging times, but the prediction is 57% too high for the 1-h averaging time. The ISC model tends to underpredict by about 25–30% for the 3- and 24-h averaging times, but is 25% high for the 1-h averaging time.
- Looking at all hours of the year, the values of the "factor of two" statistic and the correlation for the HPDM model are better than those for the ISC model at the Baldwin site. The HPDM predictions are within a factor of two of the observed concentrations about three times as often as ISC's predictions are. HPDM's correlations with observed values range from 0.42 to 0.53 (depending on averaging time), over 50% higher than ISC's correlation.
- There is little significant difference between the HPDM and ISC values of the "factor of two" statistic and the correlation at the Summit County site. This uncertainty is attributed to the fact that the two sites used for meteorological data, the stack locations and the monitoring sites are scattered over a 1000 km area, and it is likely that the input data are not representative of the entire region.
- The HPDM model does a slightly better job than the ISC model of simulating the meteorological conditions associated with the highest five observed hourly concentrations at Baldwin and Summit County.

There are a few major recommendations that follow from this analysis. They are all based on the fact that, in the past, theoretical analyses of turbulence and dispersion in the atmospheric boundary layer have emphasized certain specific ranges of conditions, such as the period during the morning when the boundary layer is rapidly growing. However, in practice, a model such as HPDM must be applied to all hours of the year.

Recommendation 1: Theoretical models should be developed for turbulence and dispersion in the afternoon, when the boundary-layer is gradually collapsing.

Recommendation 2: Dispersion in the nighttime boundary-layer is observed to result in high-ground-level concentrations for stacks with elevations of 50–100 m during periods when nocturnal jets are likely to form. More work is needed in the development of models for these conditions.

Recommendation 3: Boundary-layer observation programs are needed in which winds, temperatures and turbulence are measured at heights up to 2000 m for all hours of the year. The resulting data can be used to develop empirical profile formulae for use at other sites. Data are especially needed at heights above the nocturnal mixed layer and during the late afternoon.

Recommendation 4: With the advent of advanced satellite measurements of parameters such as surface temperature and moisture, uniform methods should be developed for assimilating this information into the surface flux equations described in Section 2, for use at routine sites across the U.S.A.

Acknowledgements—This research was sponsored by the Electric Power Research Institute, with Dr Charles Hakkarinen as the project manager. Mr Richard Osa of Science and Technology Management Inc., Mr Bruce Turner of Trinity Consultants, and Mr Robert Paine of ENSR Inc. provided much guidance and reviewed earlier drafts of this manuscript. Mr Paine also supplied the input data for the Baldwin and Summit County sites.

REFERENCES

Auer A. H. (1978) Correlation of land use and cover with meteorological anomalies. *J. appl. Met.* **17**, 636–643.

Briggs G. A. (1975) Plume rise predictions. In *Lectures on Air Pollution and Environmental Impact analysis*, pp. 59–111. American Meteorological Society, Boston, MA.

Briggs G. A. (1985) Analysis parameterizations of diffusion—the convective boundary layer. *J. Clim. appl. Met.* **24**, 1167–1186.

Businger J. A., Wyngaard J. C., Izumi Y. and Bradley E. F. (1971) Flux-profile relationships in the atmospheric surface layer. *J. atmos. Sci.* **28**, 181–189.

Carruthers D., Thomson, D., Britter R. E. and Hunt J. C. R. (1992) Description of the United Kingdom Atmospheric Dispersion Modeling System (ADMS). In *Proc. CEC Workshop on Objectives for Next Generation of Practical Short-range Atmospheric Dispersion Models*. Riso National Laboratory, Denmark.

Carson D. J. (1973) The development of a dry inversion-capped convectively unstable boundary layer. *Q. JlR. Met. Soc.* **99**, 450–467.

Caughey S. J. (1982) Observed characteristics of the atmospheric boundary layer. In *Atmospheric Turbulence and Air Pollution Modeling* (edited by Nieuwstadt F. T. M. and Van Dop H.), pp. 107–158. Reidel, Dordrecht.

Doll D., Ching J. K. S. and Kaneshire J. (1985) Parameterization of subsurface heating for soil and concrete using new radiation data. *Boundary-Layer Met.* **32**, 351–372.

Golder D. (1972) Relations between stability parameters in the surface layer. *Boundary-Layer Met.* **3**, 46–58.

Gryning S. E., Holtslag A. A. M., Irwin J. S. and Sivertsen B. (1987) Applied dispersion modeling based on meteorological scaling parameters. *Atmospheric Environment* **21**, 79–89.

Hanna S. R. (1983) Lateral turbulence intensity and prime meandering during stable conditions. *J. Clim. appl. Met.* **22**, 1424–1430.

Hanna S. R. (1989) Confidence limits for air quality models, as estimated by bootstrap and jack-knife resampling methods. *Atmospheric Environment* **23**, 1385–1395.

Hanna S. R. (1986) Lateral dispersion from tall stacks. *J. Clim. appl. Met.* **25**, 1426–1433.

Hanna S. R. and Chang J. C. (1991) Modification of the Hybrid Plume Dispersion Model (HPDM) for urban conditions and its evaluation using the Indianapolis data set. Final report prepared for Electric Power Research Institute, Palo Alto, CA.

Hanna S. R. and Chang J. C. (1992) Boundary-layer parameterizations for applied dispersion modeling over urban areas. *Boundary-Layer Met.* **58**, 229–259.

Hanna S. R. and Paine R. J. (1987) Convective scaling applied to diffusion of buoyant plumes. *Atmospheric Environment* **21**, 2153–2162.

Hanna S. R. and Paine R. J. (1989) Hybrid Plume Dispersion Model (HPDM) development and evaluation. *J. appl. Met.* **28**, 206–224.

Hicks B. B. (1985) Behavior of turbulence statistics in the convective boundary layer. *J. Clim. appl. Met.* **24**, 607–614.

Holtslag A. A. M. and van Ulden A. P. (1983) A simple scheme for daytime estimates of the surface fluxes from routine weather data. *J. Clim. appl. Met.* **22**, 517–529.

Hunt J. C. R. (1982) Diffusion in the stable boundary layer. In *Atmospheric Turbulence and Air Pollution Modeling* (edited by Nieuwstadt F. T. M. and Van Dop H.), pp. 231–274. D. Reidel, Dordrecht.

Irwin J. S. and Paumier J. O. (1990) Characterizing the dispersion state of convective boundary layers for applied dispersion modeling. *Boundary-Layer Met.* **53**, 267–296.

Nieuwstadt F. T. M. (1981) The steady-state height and resistance laws of the nocturnal boundary layer: theory compared with Cabauw observations. *Boundary-Layer Met.* **20**, 3–17.

Nieuwstadt F. T. M. (1992) A large-eddy simulation of a line source in a convective atmospheric boundary layer—I. Dispersion characteristics. *Atmospheric Environment* **26A**, 485–495.

Nieuwstadt F. T. M. and Valk J. P. (1987) A large-eddy simulation of buoyant and non-buoyant plume dispersion in the atmospheric boundary layer. *Atmospheric Environment* **21**, 2573–2587.

Olesen H. R. (1988) User's Guide for OML-Point. An air pollution model for point sources. MST LUFT-A 125, National Agency of Environmental Protection, Roskilde, Denmark.

Panofsky H. A., Tennekes H., Lenschow D. H. and Wyngaard J. C. (1977) The characteristics of turbulent velocity components in the surface layer under convective conditions. *Boundary-Layer Met.* **11**, 355–361.

Pasquill F. (1976) Atmospheric dispersion parameters in Gaussian plume modeling: part II. Possible requirements for change in the Turner Workbook Values. Report EPA-600/4-76036, U.S. Environmental Protection Agency, Research Triangle Park, NC.

Stull R. B. (1988) *An Introduction to Boundary Layer Meteorology*. Kluwer, Boston, MA.

TRC (1986) Urban power plant plume studies. EPRI Report EA-5468, research project 2736-1, Prepared by TRC, East Hartford, CN, for EPRI, Palo Alto, CA.

Uno I., Wakamatsu S., Ueda H. and Nakamura (1988) An observational study of the structure of the nocturnal urban boundary layer. *Boundary-Layer Met.* **45**, 59–82.

Venkatram A. (1988) Dispersion in the stable boundary layer. In *Lectures in Air Pollution Modeling* (edited by Venkatram A. and Wyngaard J. C.), pp. 229–266. American Meteorological Society, Boston, MA.

Wang I. T. and Chen P. C. (1980) Estimation of heat and momentum fluxes near the ground. In *Proc. 2nd Joint Conf. Applications on Air Pollution Meteorology*, pp. 764–769. American Meteorological Society, Boston, MA.

Weil J. C. (1988) Dispersion in the convective boundary layer. In *Lectures in Air Pollution Modeling* (edited by Venkatram A. and Wyngaard J. C.), pp. 167–188. American Meteorological Society, Boston, MA.

Weil J. C. (1991) Discussion of lofting model and related dispersion models. Appendix C of report by Hanna and Chang (1991).

Weil J. C. (1992) Updating the ISC model through AERMIC. 85th Annual Meeting of Air and Waste Management Association, Kansas City, MO.

Weil J. C. and Brower R. P. (1983) Estimating convective boundary layer parameters for diffusion applications. Report PPSP-MP-48 Prepared by Environmental Center, Martin Marietta Corporation, for Maryland Department of Natural Resources, Armapolis, MD.

Weil J. C. and Brower R. P. (1984) An updated Gaussian plume model for tall stacks. *J. Air Pollut. Control Ass.* **34**, 818–827.

Weil J. C. and Corio L. A. (1988) A modification of the PPSP dispersion model for highly buoyant plumes. Report PPSAP-MP-50 Maryland Power Plant Research Program, Maryland Department of Natural Resources, Annapolis, MD.

Wyngaard J. C. (1988) Structure of the PBL. In *Lectures on Air Pollution Modeling* (edited by Venkatram A. and Wyngaard J. C.), pp. 9–62. American Meteorological Society, Boston, MA.